J Appl Electrochem (2009) 39:1509–1516
DOI 10.1007/s10800-009-9832-3

ORIGINAL PAPER

Electroreduction of oxygen over iron macrocyclic catalysts for DMFC applications

Alexey Alexandrovich Serov · Myoungki Min · Geunseok Chai · Sangil Han · Sang Joon Seo · Younggil Park · Ho Kim · Chan Kwak

Received: 28 September 2008 / Accepted: 8 February 2009 / Published online: 22 February 2009

Abstract The performance of macrocyclic catalysts in oxygen reduction was investigated for a direct methanol fuel cell. The dependence of catalytic activity on different factors was determined for two classes of precursors; namely, iron porphyrin (Fe-PC) and iron phthalocyanine (Fe-TPP). It was found that there was an optimal heat-treating temperature for each precursor. Heat-treated Fe-TPP shows maximum activity at 750 °C, while the highest performance in the case of Fe-PC is observed at 500 °C. It was shown that oxygen reduction activity is affected by the number of nitrogen bonds formed with iron, particle size, and formation of carbon layers.

Keywords Fuel cell · Oxygen reduction · Iron · Catalyst

1 Introduction

A direct methanol fuel cell (DMFC) as a possible energy source for portable applications has received significant attention in recent years. Although present-day lithium–ion batteries can often meet the power density requirements of portable devices, the energy density of this type of battery is very low, permitting battery-powered micro devices to be operated for only limited periods of time. In contrast to batteries, methanol has exceptionally high energy density, therefore DMFC technology appears to be ideal for small power generation.

A. A. Serov · M. Min · G. Chai · S. Han · S. J. Seo · Y. Park · H. Kim · C. Kwak (✉)
Corporate R&D Center, Samsung SDI, Shin-dong 575, Yeongtong-gu, Suwon-si, Gyeonggi-do 443-731, South Korea
e-mail: c.kwak@samsung.com

In the early days, research in the field of fuel cells addressed fundamental aspects, but now the emphasis has shifted from academic studies to commercial applications. One of the main problems with commercial use of fuel cells is the high cost of materials such as catalyst, stack components, etc. The high price of platinum and platinum-based alloys is a major contributor to the final cost of a fuel cell. Reduction of the amount of platinum using a new preparation method [1, 2] offers a solution, but a membrane electrode assembly (MEA) with only a small amount of platinum has shown a low level of performance and significant power decrease in durability tests.

There have been many investigations of non-platinic catalysts for oxygen reduction, and there is a wide range of non-metallic materials that can substitute platinum. At present, the non-platinic catalysts for oxygen reduction reaction (ORR) can be divided into two classes: (1) the Ru or Pd-based catalysts [3–5]; (2) and derivatives of transition metal macrocyclic compounds [6–14]. Iron or cobalt complexes of porphyrins, phthalocyanine or tetra-azannulene have been reported as showing considerable promise. Although the exact active species of metallic macrocycles is not known, it is generally accepted that pyrolysis of the complexes enhances the oxygen reduction activity.

The activity of transition metal macrocyclic compounds is lower than that of platinum; however, it should be noted that non-platinic catalysts possess a number of advantages that can compensate for the weak points. When methanol crosses from the anode to the cathode, it produces a drop in potential at the cathode. The transition metal macrocyclic compounds are methanol-tolerant; accordingly, they do not produce a mixed potential at the cathode. In the case of a hydrogen fuel cell, the transition metal macrocyclic compounds can serve as the anode catalyst because they are not

sensitive to poisonous admixtures like carbon monoxide, sulfur-containing derivatives, or nitrogen compounds [14].

For all the advantages of non-platinic catalysts, the price competitiveness is the main motive power for research into the commercial use of DMFC. In the present study, two promising non-platinic precursors, iron tetraphenylporphyrin (TPP) and iron phthalocyanine (PC), were selected and examined. The temperature of heat treatment was changed in order to find the optimum preparation conditions for both precursors. This work is particularly concerned with the effect of preparation conditions on the catalyst structure of the iron macrocyclic compounds and their performance. A series of such catalysts were prepared, tested for oxygen reduction in half-cells as well as in fuel cells, and characterized by transmission electron microscopy (TEM), X-ray photoelectron spectroscopy (XPS), and thermogravimetry (TG).

2 Experiment

2.1 Preparation of catalysts

Metaloporphyrins ($C_{44}H_{28}MH_4$, M: Fe, Co, Ni, Cu, Mn, Zn) and iron phthalocyanine ($C_{32}H_{16}FeN_8$) were purchased from Aldrich. A known amount of a metalomacrocycle precursor was dissolved in 150 mL of benzene. A carbon support (Ketjen black) was added to the solution with constant mixing. The solids were dried in a rotary evaporator at 70 °C, dried again in air at 100 °C for 12 h, and calcined in argon for 4 h. The prepared catalysts contained 2 wt.% metal for half-cell test and 6 wt.% metal for single cell test. They were designated as M(X)Y, M denoting the type of metal, X denoting the type of macrocycle, and Y denoting the temperature of the heat treatment (in °C).

2.2 Rotating disk electrode

The oxygen reduction reaction over the macrocyclic electrocatalyst was studied using a rotating disk electrode. Working electrodes were prepared by mixing 11 mg of the macrocyclic electrocatalyst, 1.13 mL of water, and 1.13 mL of isopropyl alcohol. The mixture was sonicated before a small volume (13.1 μL) was applied onto a glassy carbon disk with a sectional area of 0.283 cm^2. After drying the droplet at room temperature, 11.2 μL of a Nafion® monomer solution (0.5 wt%; Dupont) was applied onto the film. The experimental setup involved a three-electrode arrangement connected to a potentiostat/galvanostat (Autolab model PGSTAT30). The reference electrode was Ag/AgCl and the counter-electrode was a platinum mesh. The electrochemical reductions were performed by rotating the catalyst-loaded electrodes at 2000 rpm at a scan rate of 10 mV s^{-1} in 50 mL of 0.5 mol L^{-1} H_2SO_4 at 25 °C.

2.3 Characterization

Samples for TEM were prepared by grinding and successive ultrasonic treatment in isopropyl alcohol for 1 min. A drop of the suspension was dried on a standard TEM sample grid covered with holey carbon film. Tecnai^{TM} G^2TEM with FEG was used for observations. Images were recorded with a Multiscan camera.

The XPS measurements were performed with an ESCALAB250 (VG Scientific, England) system using monochromatic Al-Kα radiation (1486.6 eV). Powder samples were mounted on pre-cleaned indium foils.

2.4 Single cell test

The membrane electrode assemblies (MEAs) were fabricated by spraying the catalyst ink onto Nafion 112. The anode catalyst was PtRu black (Johnson Matthey) and the cathode catalysts were Fe(TPP)Y. The Nafion content were 15 wt.% in the anode and 30 wt.% in the cathode. The catalyst-coated membrane was sandwiched between the anode gas diffusion layer (GDL, SGL 10AC) and the cathode GDL (SGL 31BC) and then the assemblies were hot-pressed under a specific load of 140 kgf cm^{-2} for 3 min at 125 °C.

Polarization curves were obtained by the Wonatech testing system using a homemade single cell with a working area of 10 cm^2. Methanol solution (1 mol L^{-1}) was fed to the anode side of the cell (anode stoichiometry = 3) while dry air was fed to the cathode side (cathode stoichiometry = 3) under atmospheric pressure. The single cell was operated at 80 °C.

3 Results

3.1 Rotating disk electrode

The polarization curves for oxygen reduction on heat-treated macrocycles with different central ions are shown in Fig. 1. The electrochemical reaction seems to be under kinetic and diffusion control in the whole potential region. A limiting diffusion current is not reached at a cathodic potential of 0.30 V/NHE for the catalysts. Over iron and cobalt, oxygen reduction starts above 0.7 V and increases the catalytic current, with the potential moving in a negative direction. Apparently, four other central metals, such as Mn, Zn, Ni, and Cu, show much lower catalytic activities. This result is in accord with the general trends in macrocyclic

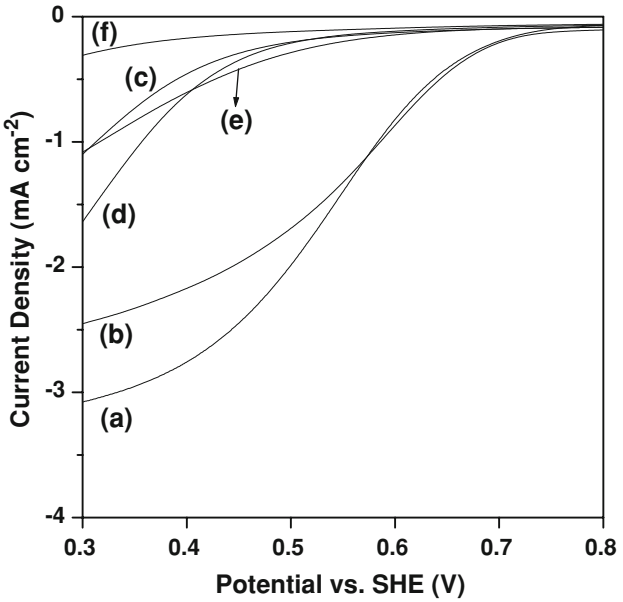

Fig. 1 Steady-state polarization curves for oxygen reduction in 0.5 mol L^{-1} H_2SO_4 solution on RDE prepared with (a) Fe(TPP)1000, (b) Co(TPP)1000, (c) Ni(TPP)1000, (d) Cu(TPP)1000, (e) Mn(TPP)1000, and (f) Zn(TPP)1000

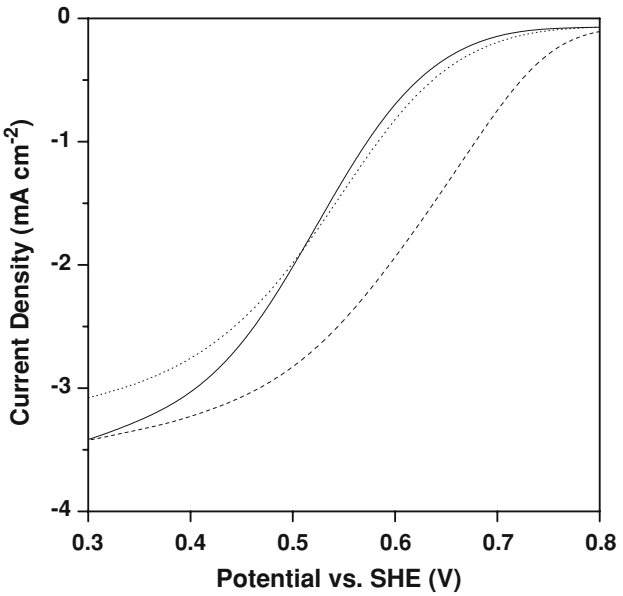

Fig. 2 Steady-state polarization curves for oxygen reduction in 0.5 mol L^{-1} H_2SO_4 solution on RDE prepared with Fe(TPP)500 (*continuous*), Fe(TPP)750 (*broken*), and Fe(TPP)1000 (*dotted*)

catalyst research. In the case of phthalocyanines, the order of Fe > Co > Ni > Cu has been reported [15].

The dependence of the reduction reaction as a function of the potential and heat-treatment temperature on the iron tetraphenylporphyrin (Fe-TPP) and the iron phthalocyanine (Fe-PC) catalysts are shown in Figs. 2 and 3. Similar to Fig. 1, the electrochemical reaction is under kinetic and

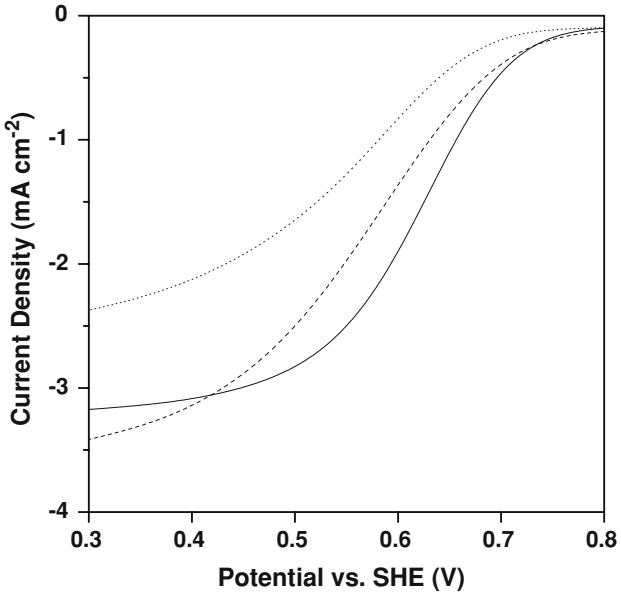

Fig. 3 Steady-state polarization curves for oxygen reduction in 0.5 mol L^{-1} H_2SO_4 solution on RDE prepared with Fe(PC)500 (*continuous*), Fe(PC)750 (*broken*), and Fe(PC)1000 (*dotted*)

diffusion control in the whole range, but a limiting diffusion current is nearly reached. Heat-treatment of Fe-TPP supported on carbon in an inert atmosphere enhances the oxygen reduction activity up to 750 °C, but an increase above that temperature reduces the activity. In contrast, the oxygen reduction activity decreases continuously with increasing temperature of the heat-treatment in the case of Fe-PC supported on carbon.

3.2 Thermogravimetry

The thermogravimetric results of Fe-TPP and Fe-PC precursors are plotted in Fig. 4. The profiles for Fe-TPP can be divided according to the temperature regions for the characteristic weight loss. (i) A small initial weight loss is observed up to ~400 °C. (ii) Major weight loss occurs from 400 to 530 °C, due to the destruction of ligand structure. (iii) Further decrease of weight occurs gradually above 530 °C. In contrast, Fe-PC is decomposed in large part in region (ii), and shows a plateau above 530 °C.

3.3 TEM

The HAADF TEM images of the Fe-TPP samples indicate the extent of agglomeration of the samples as shown in Fig. 5. For Fe(TPP)500, agglomerated particles are not observed. However, dot-shaped shining particles are seen for Fe(TPP)750, suggesting the presence of large particles. The population of large particles is greatly increased for Fe(TPP)1000.

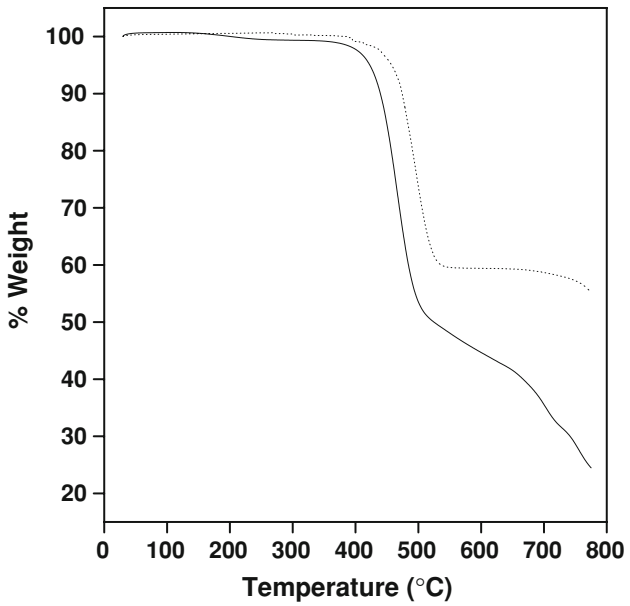

Fig. 4 TGA profiles of iron tetraphenylporphyrin (*continuous*) and iron phthalocyanine (*dotted*)

Bright-field images of the samples could be observed in the special regions where one separate particle is present in the form of island. The images of Fe(TPP)750 and Fe(TPP)1000 shown in Fig. 6 do not represent the overall particle size distribution. It appears that the particles are covered with a polymerized carbon layers in both samples. The thickness of polymerized carbon layer in Fe(TPP)750 is estimated as 6–8 nm, however the border line of the carbon layer is unclear (Fig 6b), whereas that of Fe(TPP)1000 is estimated as 10–12 nm. As can be seen in Fig. 6b and d, the polymerized carbon layers of Fe(TPP)750 have a low level of graphitization, while the carbon layers of Fe(TPP)1000 show a well-ordered graphitic character. Several studies have reported that metal catalyzed the formation of carbon layer [16–18]. The carbon species is unstable at high temperatures, therefore agglomeration of metal can occur. In the subsequent step, laminar graphite is formed at the surface of iron. Potoczna-Petru has reported that the unordered carbon dissolved in metal precipitates even in the cooling stage [17].

The particle sizes of the Fe-PC catalysts depend on calcination temperature to a smaller extent than those of the Fe-TPP catalysts, as can be seen in Fig. 7. There is small change in the microstructure of the Fe-PC catalysts after heating the sample at 750 and 1000 °C although a few large particles appear in the TEM images.

3.4 X-ray photoelectron spectroscopy

Figures 8 and 9 present the XP spectra of nitrogen measured for Fe(TPP)Y and Fe(PC)Y, respectively. The binding

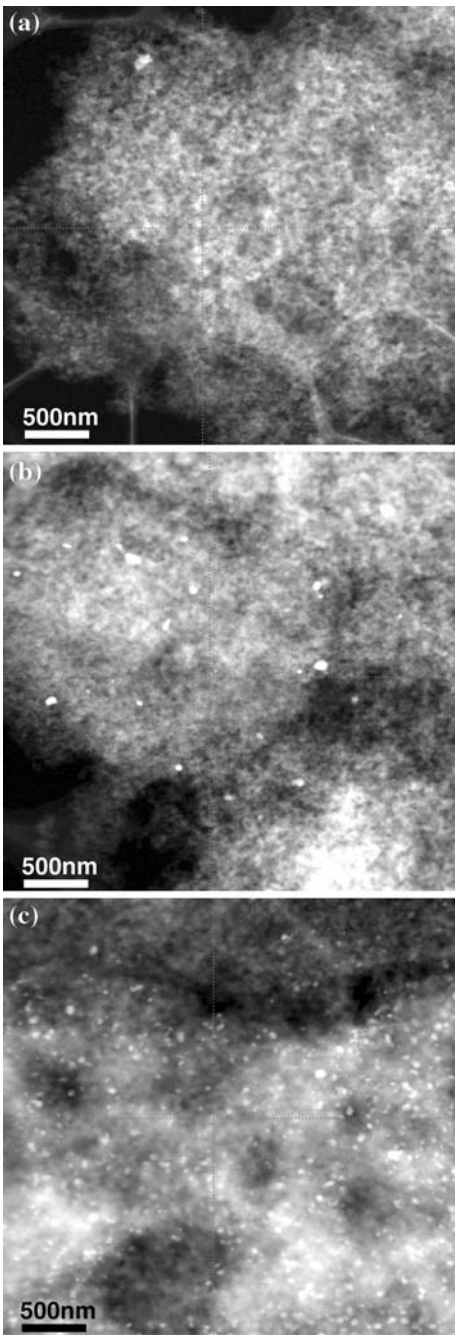

Fig. 5 HAADF images of **a** Fe(TPP)500, **b** Fe(TPP)750, and **c** Fe(TPP)1000

energy values for the N 1 s peak appear at about 398.5 and 400–401 eV. In a study of nitrogen-containing carbon materials without metal [16], peaks at 398.6(±0.3) eV, 400.5(±0.3) eV, and 401.3(±0.3) eV were assigned to pyridinic, pyrrolic, and quaternary nitrogen, respectively. In another study of polymers containing nitrogen and iron [19], the peak centered at 397.7 eV was assigned to the iron-nitrogen bond. In this study, the low binding energy peak is assigned to the sum of two types of nitrogen. One is an

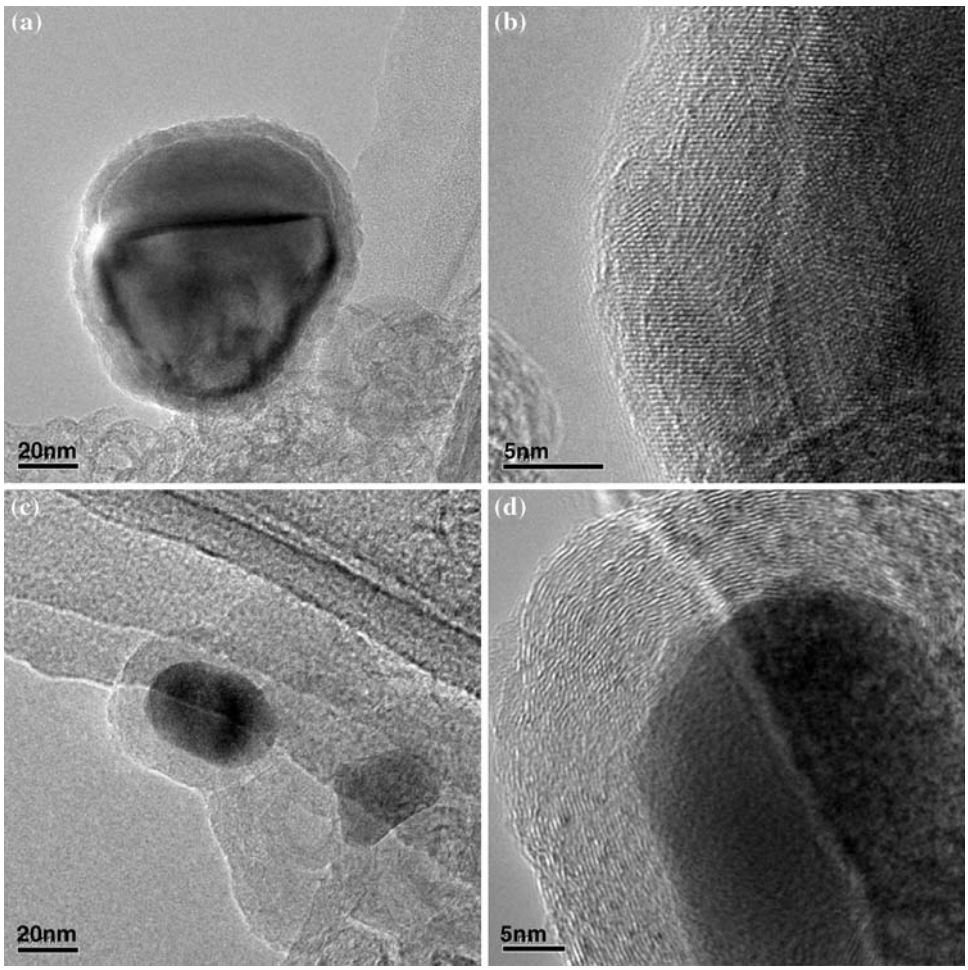

Fig. 6 Bright-field images of **a**, **b** Fe(TPP)750, and **c**, **d** Fe(TPP)1000

incompletely decomposed nitrogen species interacting with iron and the other is pyridinic-type nitrogen without interaction with iron, which is produced during the heat treatment. The high binding energy peak is assigned to the carbon-nitrogen species containing pyrrolic and quaternary-type nitrogen.

With increasing temperature of the heat treatment, two types of change are observed in the N 1 s band of both Fe(TPP)Y and Fe(PC)Y. One is the enhancement of the high-energy peak accompanied by reduction of the low-energy peak, and the other is the characteristic peak shift, i.e. the high-energy peak to higher binding energies. These changes in the N 1 s bands occur due to formation of the active species and the formation of carbon layers outside the metal particles.

3.5 MEA performance

The single cells were activated for four days to achieve the maximum performance of them. The cells were run at the operation temperature at 0.2 V for 2 h everyday. 1 mol L^{-1} methanol was put in the anode during the keeping at room temperature. No degradation of the performance was observed in the activation procedures. It is known that macrocyclic compounds are stable in acidic media [20].

Figure 10 shows the single-cell performance of Fe(TPP)Y. The open-circuit voltage (OCV) of the fuel cell is around 0.70–0.76 V for the MEAs. The cell prepared using Fe(TPP)750 achieves a peak power density of 28 mW cm^{-2}, whereas the cell with other catalysts shows around 20 mW cm^{-2} at 80 °C. This MEA performance is in good agreement with the RDE results with the sample calcined at different temperatures. The peak power density of platinum black catalysts in our experimental system is around 125 mW cm^{-2} which is much higher than those of macrocyclic catalysts. The metal loading of macrocyclic catalysts (0.5 mg cm^{-2}) is lower than that of the platinum catalyst (4 mg cm^{-2}). Low metal content in MEA is the main reason of low performance. Large volume of macrocyclic compound prevents the loading increase within the limited space of the effective volume in the MEAs.

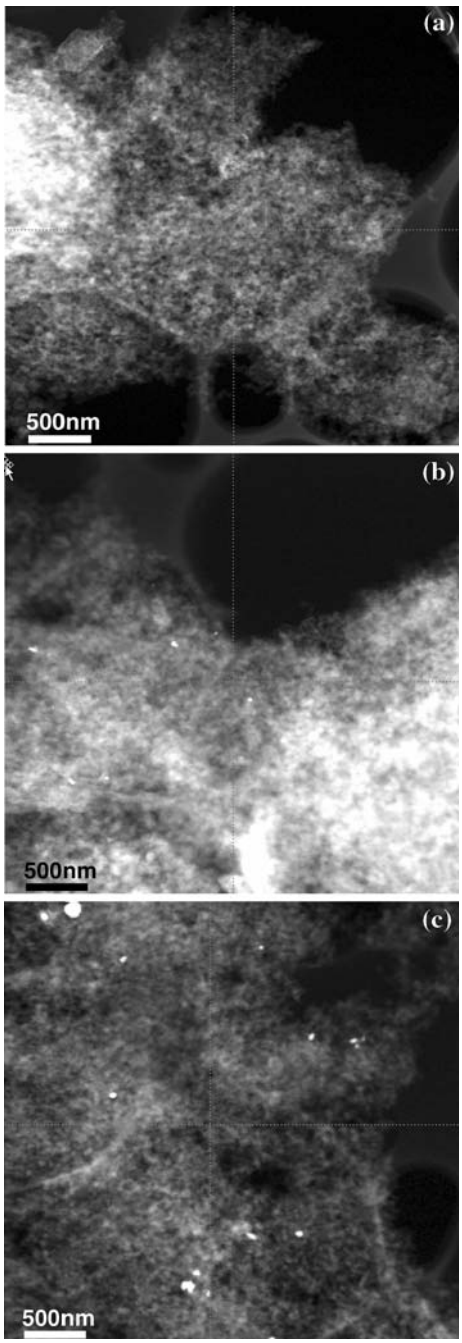

Fig. 7 HAADF images of **a** Fe(PC)500, **b** Fe(PC)750, and **c** Fe (PC)1000

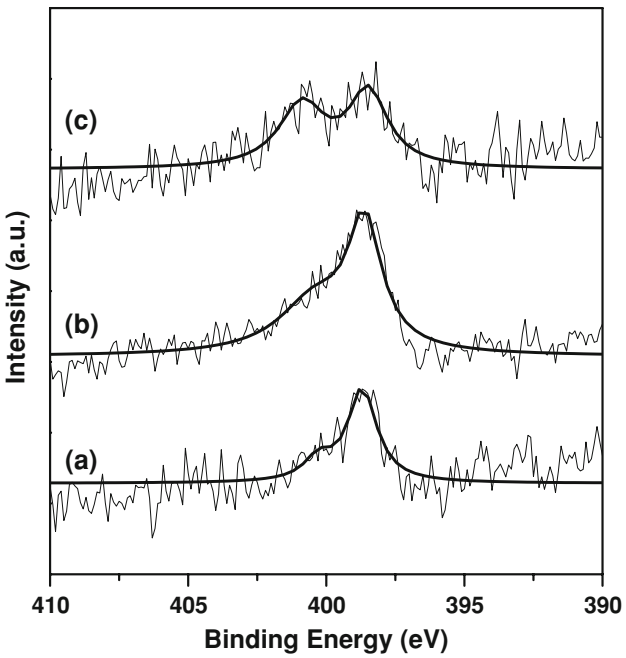

Fig. 8 XP spectra of N 1 s for **a** Fe(TPP)500, **b** Fe(TPP)750, and **c** Fe(TPP)1000

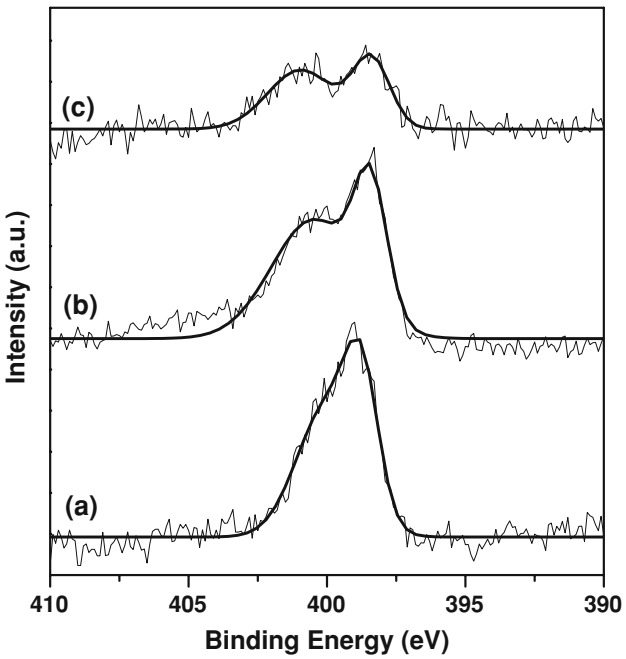

Fig. 9 XP spectra of N 1 s for **a** Fe(PC)500, **b** Fe(PC)750, and **c** Fe(PC)1000

4 Discussion

4.1 Changes in active species during the heat treatment

In addition to the low oxygen reduction activity of non-noble metals, a lack of stability in the acidic medium of polymer electrolyte fuel cells prevents the use of them for DMFC, although they are widely used as active components in many fields of catalysis. Heat treatment at high temperature can provide higher stability of the macrocyclic catalyst in acidic media [21]. Dense and well-ordered crystalline carbon layers observed by TEM can protect the catalytic centers from acid media.

Despite different points of view on the catalytic properties of macrocyclic compounds, it is generally believed

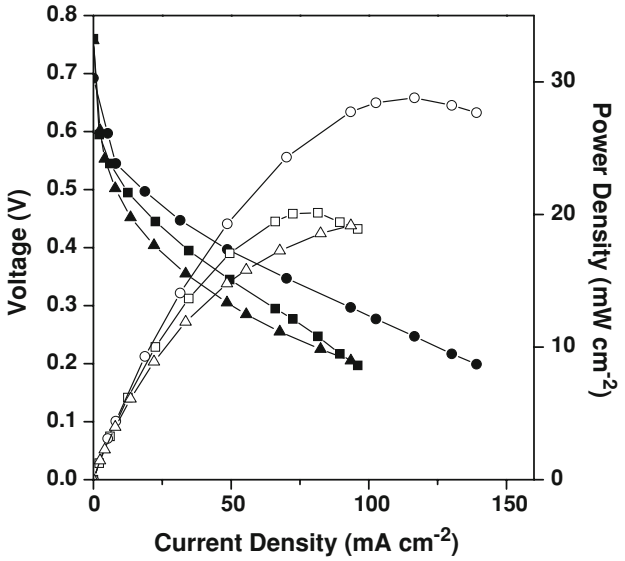

Fig. 10 The polarization curves and power density curves of single cells with Fe(TPP)500 (*square*), Fe(TPP)750 (*circle*), and Fe(TPP)1000 (*triangle*). Fuel: 1 mol L^{-1} methanol (stoichiometry = 3); oxidant: air under atmospheric pressure (stoichiometry = 3); temperature: 80 °C

that the central metal atom plays an important role in the oxygen reduction reactions. As shown in Fig. 1, iron and cobalt have much higher activities than other metals, which supports the importance of central metals. Fe(TPP)1000, where the active species are covered with graphitic carbon layers, can also reduce oxygen catalytically. It is reported that a nitrogen-containing carbon compound itself shows oxygen reduction activity [16]. To sum up, the main active site for oxygen reduction is the metal–nitrogen species, which can be written as N_x-iron species. However, the carbon–nitrogen species also has appreciable oxygen reduction activity.

With increasing temperature of the heat treatment, several changes in the macrocyclic catalysts occur, as observed in the results of thermogravimetry, TEM, and XPS studies. They are: (i) weight loss attendant upon the precursor decomposition; (ii) formation of the active species; (iii) particle size growth due to agglomeration of the metal particles; and (iv) coverage by graphite-like carbon layers. These phenomena appear in different aspects, depending on the type of macrocycle.

Fe-TPP loses weight continuously with increasing temperature, accompanied by the removal of the chelate group and changes in the active species. Particle size increases to a great extent with increasing temperature. Polymerized carbon layers can be observed in large particles, but it is assumed that the carbon layers are present also in small particles. In the XP spectra, the low-energy peak of Fe(TPP)750, representing the iron-nitrogen species and carbon-nitrogen species in a pyridinic form, does not decrease markedly compared with that of Fe(TPP)500. The nitrogen atoms separated from iron may form pyridinic carbon-nitrogen species, which can show catalytic activity of oxygen reduction. As shown in Fig. 6, the carbon layers of Fe(TPP)750 have a relatively amorphous character, whereas those of Fe(TPP)1000 seem to be graphite-like carbon. The formation of graphite-like carbon in Fe(TPP)1000 is consistent with the increase of the higher energy peak in the XP spectra of Fe(1000), which represents the quaternary type of carbon-nitrogen species.

In the case of Fe-PC, a slight weight loss occurs above 530 °C, suggesting that most of the chelate groups decompose below this temperature. Although the weight of Fe-PC does not change greatly between 500 and 750 °C, changes in the active species occur in this temperature region, as shown by the different XP spectra. At 750 °C, the peak at 400.6 eV representing the quaternary type of carbon-nitrogen species appears in considerable amounts. Large particles are observed in the samples calcined at high temperatures; however, the extent of the agglomeration is relatively small compared with that of Fe-TPP. The earlier finish of decomposition reduces the period in which the sample is unstable.

4.2 Catalytic activity

As shown in Figs. 2 and 3, Fe-TPP shows maximum activity at 750 °C, whereas an increase of the temperature reduces the overall performance of oxygen reduction in the case of Fe-PC. Fe(TPP)750 shows higher oxygen reduction activity than Fe(TPP)500 in spite of the large particle size observed by TEM. Production of a new highly active species could be the reason. Between 500 and 750 °C, weight loss of Fe-TPP occurs continuously, which suggests a gradual breakage of iron–nitrogen bonds. There should be an optimum number of nitrogen-iron bonds that can form the most active phase. We believe that a highly active species is produced at 750 °C, although the formation of highly active species is not observed in the XP spectra due to the similar binding energies of the iron–nitrogen species and the pyridinic carbon–nitrogen species. The relatively amorphous carbon layer is porous [22] and, therefore, the blockage of oxygen by the carbon layer is not great. Pyridinic nitrogen sites on the amorphous carbon layer could also act as active sites.

The oxygen reduction activity is decreased for Fe(TPP)1000. Analysis of TEM images shows that treatment at 1000 °C increases the particle size and the graphitization of the carbon layers around the surface of Fe–N particles. The crystalline carbon layer covering the surface of the metal-nitrogen is dense and, therefore, it inhibits the access of oxygen to the active center. The quaternary type carbon-nitrogen species on the crystalline carbon layer does not act as an active center.

In the case of Fe-PC, full decomposition of the precursor takes place by around 500 °C, which means the formation of active centers is finished at this temperature. Further increase of the temperature gives rise to the agglomeration of the catalytic particles and the production of the quaternary type carbon–nitrogen species, as shown by the TEM and XPS results. Accordingly, the catalytic activity for oxygen reduction is decreased with an increase of temperature beyond 500 °C.

5 Conclusions

On the basis of the experimental observations and the discussion above, we reach the following conclusions about the iron macrocyclic catalysts and catalytic behavior in the electroreduction of oxygen. Heat treatment of the macrocyclic catalysts causes weight loss, formation of the active phase, coverage by carbon layers, and growth of particle size. These changes appear in different ways, depending on the precursor type. Heat-treated Fe-TPP shows maximum activity at 750 °C, while the highest performance is observed at 500 °C in the case of Fe-PC. The oxygen reduction activity is affected by the number of nitrogen atoms bonding with iron, particle size, and the formation of carbon layers.

References

1. Ye S, Vijh A, Dao L (1996) J Electroanal Chem 415:115
2. Fournier J, Faubert G, Tilquin JY, Cote R, Guay D, Dodelet JP (1997) J Electrochem Soc 144:145
3. Bron M, Bogdanoff P, Fiechter S, Dorbandt I, Hilgendorff M, Schulenburg H, Tributsch H (2001) J Electroanal Chem 500:510
4. Shukla AK, Raman RK (2003) Annu Rev Mater Res 33:155
5. Fernandez JL, Raghuveer V, Manthiram A, Bard AJ (2005) J Am Chem Soc 127:13100
6. Jahnke H, Schonbron M, Zimmerman G (1976) Top Curr Chem 61:133
7. Bagotzky VS, Tarasevich MR, Radyushkina KA, Levina OA, Andrusyova SI (1977/78) J Power Sources 2:233
8. Ladouceur M, Ladande G, Guay D, Dodelet JP (1993) J Electrochem Soc 140:1974
9. Wiesener K, Ohms D, Neumann V, Franke R (1989) Mater Chem Phys 22:457
10. Bouwkamp-Wijnoltz AL, Visscher W, van Veen JAR (1998) Electrochim Acta 43:3141
11. Lalande G, Tamizhmani G, Cote R, Dignard-Bailey L, Trudeau ML, Schulz R, Guay D, Dodelet JP (1995) J Electrochem Soc 142:1162
12. Gouerec P, Savy M (1999) Electrochim Acta 44:2653
13. Gojkovic SLJ, Gupta S, Savinell RF (1999) J Electroanal Chem 462:63
14. Venkataraman R, Kunz HR, Fenton JM (2004) J Electrochem Soc 151:A703
15. Wiesener K, Ohms D, Neumann V, Franke R (1989) Mater Chem Phys 22:457
16. Matter PH, Zhang L, Ozkan US (2006) J Catal 239:83
17. Dignard-Bailey L, Trudeau ML, Joly A, Schulz R, Lalande G, Guay D, Dodelet JP (1994) J Mater Res 9:3203
18. Potoczna-Petru D (1991) Carbon 29:73
19. Wagner AJ, Wolfe GM, Fairbrother DH (2003) Appl Surf Sci 219:317
20. Lalande G, Faubert G, Cote R, Guay D, Dodelet JP, Weng LT, Bertrand P (1996) J Power Sources 61:227
21. Faubert G, Cote R, Dodelet JP, Lefevre M, Bertrand P (1999) Electrochim Acta 44:2589
22. Lefèvere M, Dodelet JP, Bertrand P (2002) J Phys Chem B 106:8705